Am J Cancer Res 2025;15(5):2285-2300
www.ajcr.us /ISSN:2156-6976/ajcr0165120

Original Article

Gut microbiota is associated with the disease characteristics of patients with newly diagnosed diffuse large B-cell lymphoma

Zheng Li[1], Jiajie Shi[2], Xiaolin Wu[1], Siyao Yan[3], Zhe Gao[1], Yueping Liu[4]

[1]Department of Hematology, Hebei Medical University Fourth Hospital, Shijiazhuang 050000, Hebei, China; [2]Department of Breast Surgery, Hebei Medical University Fourth Hospital, Shijiazhuang 050000, Hebei, China; [3]School of Public Health, Hebei Medical University, Shijiazhuang 050000, Hebei, China; [4]Department of Pathology, Hebei Medical University Fourth Hospital, Shijiazhuang 050000, Hebei, China

Received April 7, 2025; Accepted May 20, 2025; Epub May 25, 2025; Published May 30, 2025

Abstract: Objective: To investigate the relationship between the gut microbiota and the biological characteristics of patients with newly diagnosed diffuse large B-cell lymphoma (DLBCL). Methods: This prospective study included 71 patients with newly diagnosed DLBCL. The microbiota was analyzed using 16S ribosomal DNA sequencing of fecal samples. Blood cytokines, PD-1, and PD-L1 were measured by enzyme-linked immunosorbent assay. Stratified analyses based on clinical characteristics were conducted to investigate correlations between alterations in gut microbiota and key clinicopathological parameters of DLBCL. Results: In the analysis of gut microbiota heterogeneity (α diversity index), species abundance was significantly higher in the International Prognostic Index (IPI) < 3 group compared to the IPI ≥ 3 group (high-risk group). Ruminococcus was increased in the IPI ≥ 3 group. Parabacteroides, Ruminococcus, and Eubacterium were increased in the non-germinal center B-cell-like group, while Lachnospira was decreased. Megamonas was significantly increased in the high β2-microglobulin group, while Lactobacillus reuteri and Lachnospira were decreased. In the low CD4+/CD8+ ratio group, Parabacteroides was increased, while Akkermansia was decreased. Patients who failed to achieve complete remission at interim evaluation showed marked increases in Ruminococcus and Alistipes. Extranodal involvement was associated with elevated Alistipes and Enterococcus. Conclusions: This study identified a potential relationship between the gut microbiota and DLBCL characteristics, highlighting specific gut microbiota organisms that may influence disease development and progression.

Keywords: Gut microbiota, diffuse large B-cell lymphoma, 16S ribosomal DNA, Parabacteroides, Akkermansia, Megamonas

Introduction

Diffuse large B-cell lymphoma (DLBCL) is a highly aggressive and heterogeneous type of non-Hodgkin lymphoma [1]. Previous studies have suggested that the prognosis of DLBCL patients is influenced by factors such as cellular origin, clinical course, and molecular characteristics [2]. While various treatments are available for DLBCL, including chemotherapy, radiotherapy, immunochemotherapy, targeted therapy, and cell therapy, patient outcomes vary greatly due to individual immune differences [3, 4]. One study indicated that 30%-40% of patients develop refractory and recurrent disease after standardized first-line treatment, resulting in poor prognosis [5]. Therefore, there is an urgent need to explore the pathogenesis of DLBCL to identify new treatment strategies and improve patient outcomes.

The human body is home to tens of thousands of microorganisms, distributed across regions such as the oral mucosa, skin, gastrointestinal tract, and conjunctiva. The majority of these symbiotic microorganisms reside in the colon, where they engage in a balanced interaction with the immune system [6]. Additionally, the gut-brain axis, consisting of the enteric nervous system, hypothalamus-pituitary-adrenal axis, autonomic nervous system, and central nervous system, has garnered increasing atten-

https://doi.org/10.62347/DIMG6893

tion. One study suggested that the communication between the gut and brain, mediated by the composition and diversity of the gut microbiota, significantly influences host health [7].

Several studies have shown that the gut microbiota may be closely linked to the pathogenesis of various diseases, including inflammatory, autoimmune, metabolic, neoplastic, and neurodegenerative conditions [8-11]. However, research on the role of the gut microbiota in tumor immunity has primarily focused on gastrointestinal solid tumors, with limited exploration of lymphoma, a cancer type particularly sensitive to immune responses. Recently, Lu et al. have reported that lipopolysaccharides from the inherent microbiota of lymphoma patients synergized with tumor necrosis factor (TNF) signaling, enhancing nuclear factor-κB signaling via MyD88-dependent Toll-like receptor 4 (TLR4) signaling, thereby increasing intestinal B-cell survival and proliferation [12]. This finding may provide a fundamental basis for exploring the role of the gut microbiota in the pathogenesis of lymphoma.

This study aims to explore the relationship between the gut microbiota and antitumor immunity in untreated DLBCL patients using 16S metagenomic ribosomal DNA sequencing. The findings may provide insights into the pathogenesis of DLBCL and lay the groundwork for future interventional studies and treatment strategies.

Materials and methods

Case collection

With approval from the Ethics Committee of the Fourth Hospital of Hebei Medical University, 71 patients with newly diagnosed DLBCL, who were admitted to the Hematology Department from January 2021 to October 2021, were retrospectively enrolled. All patients provided written informed consent. The inclusion criteria were (a) patients with DLBCL confirmed by biopsy, (b) patients not treated for antitumor therapy before the diagnosis of DLBCL, (c) patients who received six to eight cycles of R-CHOP or similar treatments, and (d) patients with complete clinical data. A total of 250 patients were eligible for inclusion in the study. The exclusion criteria were (a) patients with no or incomplete histopathological data, (b) patients treated for lymphoma before the diagnosis of DLBCL, and (c) patients with other malignant tumors. Two patients had missing clinical data and were excluded, resulting in 69 patients who met the inclusion criteria for analysis. Tissue samples were obtained from all patients via biopsy or puncture of the lesion site and examined at the pathology department. DLBCL diagnosis and classification followed the World Health Organization's 2022 classification of hematopoietic and lymphoid neoplasms [13]. The samples were analyzed by at least two qualified pathologists for confirmation of the diagnosis.

Methods

Clinical data collection: DLBCL was classified into germinal center B-cell-like (GCB) and non-GCB subtypes based on immunohistochemistry using the Hans algorithm. DLBCL was staged according to the Ann Arbor staging system. The patient's physical condition and tumor burden were evaluated using the Eastern Cooperative Oncology Group and International Prognostic Index (IPI) scores. Double-expressor lymphoma (DEL) was identified by co-expression of Myc (≥ 40%) and Bcl-2 (> 50%) on immunohistochemistry, without concurrent Myc and Bcl-2 rearrangements [13]. Based on protein expression of Bcl-2 and c-Myc from immunohistochemistry, combined with fluorescence in situ hybridization, patients were categorized into DEL and non-DEL groups. All patients received standard first-line treatment with the RCHOP regimen (rituximab, cyclophosphamide, doxorubicin, vincristine, and prednisone). After four cycles of RCHOP therapy, treatment efficacy was assessed according to the Lugano lymphoma response criteria through imaging. If the criteria were met, the response was classified as complete response (CR); otherwise, it was categorized as non-CR.

Serum cytokines, PD-1, and PD-L1 measurements: Peripheral venous blood samples (4-5 mL) were collected in the morning after fasting for 8-10 hours into tubes containing sodium citrate as an anticoagulant. Serum levels of interleukin-2, interleukin-6, interleukin-10, TNF-α, and interferon-γ were measured by enzyme-linked immunosorbent assay (ELISA). PD-1 and PD-L1 were measured using the Human PD-1 ELISA Kit (Proteintech, USA) according to the manufacturer's instructions.

Fecal sample collection and DNA extraction: None of the patients had food preferences, food allergies, or had taken probiotics, antibiotics, or lipid-lowering drugs in the past 2 months. Fresh fecal samples were collected from all patients before their first treatment, 1-2 days prior to receiving the standard RCHOP regimen. Samples were placed in sterile specimen bottles, stored in a dedicated sample box, and kept at -20°C. Within 2 hours, samples were transferred to a freezer and stored at -80°C for cryopreservation. DNA was extracted from the fecal samples using a standard kit [14]. DNA quality was verified with a NanoDrop microspectrophotometer and agarose gel electrophoresis, and samples were stored at -80°C for further analysis.

16S ribosomal DNA sequencing: Genomic DNA was extracted, and the V3 + V4 region of the 16S ribosomal DNA was amplified using specific barcoded primers. Purified amplification products were ligated with sequencing adapters to construct a sequencing library, which was sequenced on the Illumina platform (Illumina Inc., USA). After obtaining raw sequencing data, FASTP software was used to filter low-quality data. FLASH (Fast Length Adjustment of SHort reads) software was used to merge paired-end reads into tags, followed by further filtering. Data obtained from TagCleaner were clustered using USEARCH software to eliminate detected chimeric tags, resulting in effective tags. The operational taxonomic unit (OTU) sequences were clustered based on 100% similarity, and OTU abundance statistics were calculated based on effective tags to facilitate subsequent analysis.

Statistical analysis: The Greengenes database (https://www.arb-silva.de/) was used as the species database [15]. α and β diversity analyses were employed to examine the diversity and homogeneity of the gut microbiota composition in DLBCL patients. The Wilcoxon rank - sum test (Q1, Q3) was used to detect the degree of differences between groups. When statistical significance was found, the Adonis test and Anosim test were employed. The upper limit of the maximum observed value (Q3 + IQR) and the lower limit of the minimum observed value (Q3 - IQR) were set. Statistical analyses of the gut microbial community structure of DLBCL patients with different biological characteristics were conducted at different taxonomic levels (phylum, class, order, family, genus, and species) of the gut microbiota to identify the differences in dominant microbial communities among different groups. A p-value of < 0.05 was considered statistically significant.

Results

Clinical features

The cohort had a median age of 64 years (range: 27-85), with a male predominance (52.17%). Advanced disease (Ann Arbor stage III/IV) accounted for 66.67% of the cases, and 24.64% of the patients presented with B symptoms (e.g., fever, night sweats, and weight loss). Immunohistochemical subtyping showed a predominance of non-germinal center B-cell-like (non-GCB) origin, accounting for 62.32% of the cases. At interim evaluation, 44.93% of patients failed to achieve complete remission (CR), with 26% progressing to relapsed/refractory DLBCL. The baseline clinical characteristics of the 69 patients are summarized in **Table 1**.

Comparison of species differences

Ann Arbor staging: Patients with DLBCL were divided into two groups: Ann Arbor stage I-II (AA1; n = 23) and Ann Arbor stage III-IV (AA2; n = 46). There were no significant differences in the α and β diversity indices between the two groups (both $P > 0.05$). Principal coordinate analysis (PCoA) based on Bray-Curtis dissimilarity at the family taxonomic level revealed distinct clustering patterns between the groups. However, subsequent permutational multivariate analysis of variance (Adonis test) and analysis of similarities showed no significant differences in gut microbiota composition ($R^2 < 0.05$, $P > 0.05$) (**Figure 1**).

IPI: The patients were grouped based on the IPI into the IPI-1 group (IPI < 3 points; n = 34) and the IPI-2 group (IPI ≥ 3 points; n = 35). The species abundance in the IPI-1 group was significantly higher than in the IPI-2 group ($P < 0.05$), but there was no significant difference in species evenness between the groups (**Figure 2A**). β diversity analysis demonstrated significant differences in the microbial community between the two groups. PCoA based on Bray-Curtis dissimilarity at the OTU level revealed distinct clustering patterns (**Figure 2B**), and the

Table 1. Baseline clinical characteristics of the enrolled patients

Clinical characteristics	Cases (n = 69)
Age (years)	
< 60	29 (42.03%)
≥ 60	40 (57.97%)
Sex	
Male	36 (52.17%)
Female	33 (47.83%)
Pathological subtype	
Non-GCB	43 (62.32%)
GCB	26 (37.68%)
DEL	
Non-DELs	34 (49.28%)
DELs	35 (50.72%)
Clinical stage	
Stage I-II	23 (33.33%)
Stage III-IV	46 (66.67%)
B-symptom	
Group A	52 (75.36%)
Group B	17 (24.64%)
LDH (μ/L)	
≥ 250	42 (60.87%)
< 250	27 (39.13%)
IPI score	
< 3 points	34 (49.28%)
≥ 3 points	35 (50.72%)
Extranodal organ involvement	
0	16 (23.19%)
1	36 (52.17%)
≥ 2	17 (24.64%)
Efficacy assessment after four courses of treatment	
CR	38 (55.07%)
NCR	31 (44.93%)
Ki67	
≥ 70%	38 (55.07%)
< 70%	31 (44.93%)
β2-MG (μg/mL)	
≥ 2.7	36 (52.17%)
< 2.7	33 (47.83%)

β2-MG, β2-microglobulin; CR, complete response; DEL, double-expressor lymphoma; GCB, germinal center B-cell-like; IPI, International Prognostic Index; LDH, lactate dehydrogenase.

Adonis test confirmed statistically significant dissimilarities (R^2 = 0.062, P = 0.0432) (**Figure 2C**). Genus-level receiver operating characteristic (ROC) curve analysis confirmed the discriminative power of key taxa, with area under the ROC curve (AUC) values exceeding 0.70 (**Figure 2D**). Differential abundance analysis identified an elevated abundance of Ruminococcus gnavus (P = 0.04) in the IPI-2 subgroup compared to the IPI-1 group (**Figure 2E-G**).

Hans algorithm: Patients were classified into GCB (n = 26) and non-GCB (n = 43) groups based on immunohistochemical subtyping. No significant differences in α diversity were found between the two groups (P > 0.05) (Supplementary Figure 1). Significant differences in microbial composition were observed between the groups based on β diversity indices. PCoA revealed distinct clustering patterns (**Figure 3A**), and the Adonis test confirmed statistically significant dissimilarities (R^2 = 0.071, P = 0.032) (**Figure 3B**). Genus-level ROC curve analysis further validated the discriminative power of key taxa, with AUC values exceeding 0.70 (**Figure 3C**). Comparison of species composition showed that Eubacterium (P = 0.03), Ruminococcus (P < 0.01), and Parabacteroides (P < 0.01) were elevated in the non-GCB group compared with the GCB group (**Figure 3D-F**).

CD4+/CD8+ ratio: Patients were divided into the high CD4+/CD8+ ratio (HCDR) group (CD4+/CD8+ ratio > 2; n = 34) and low CD4+/CD8+ ratio (LCDR) group (CD4+/CD8+ ratio < 2; n = 35). There were no significant differences in α diversity between the two groups (P > 0.05) (Supplementary Figure 2). However, in the β diversity index, PCoA based on Bray-Curtis dissimilarity revealed distinct clustering patterns (**Figure 4A**), and the Adonis test confirmed statistically significant differences (R^2 = 0.084, P = 0.0375) (**Figure 4B**). Genus-level ROC curve analysis confirmed the discriminative power of key taxa, with AUC values exceeding 0.70 (**Figure 4C**). Comparison of species composition revealed

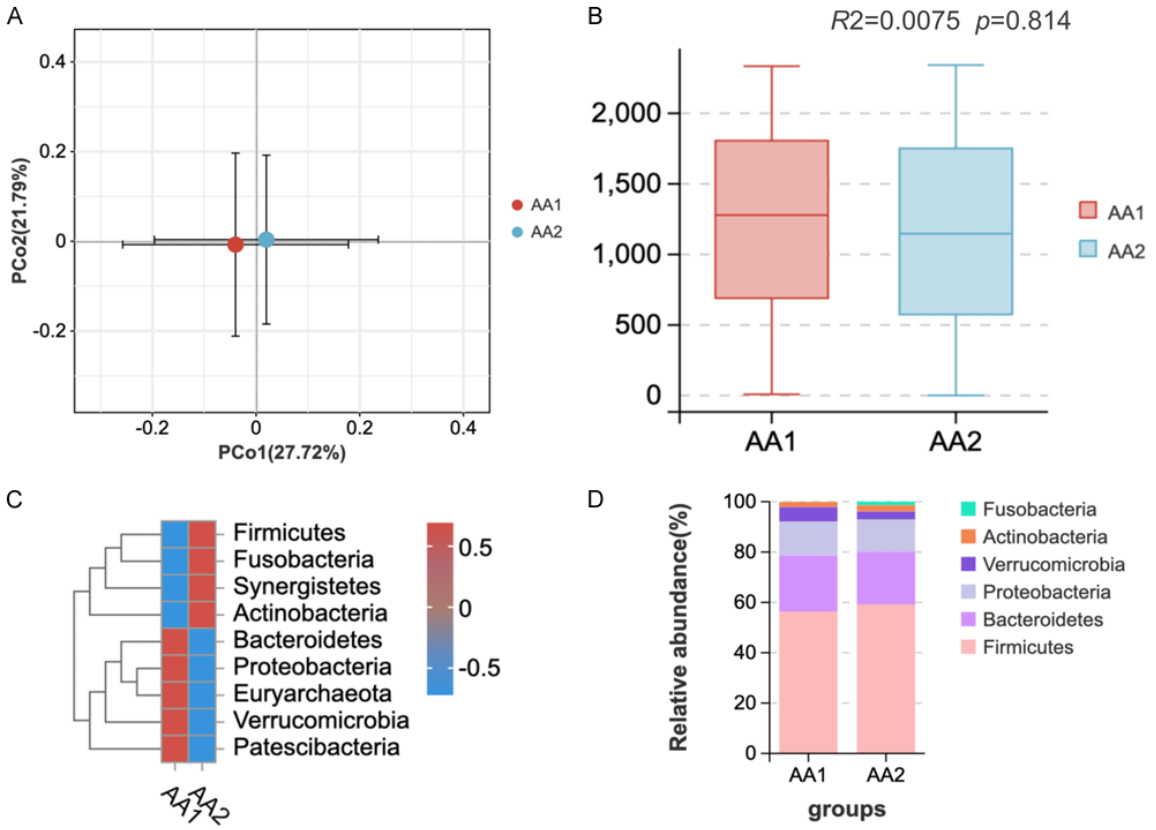

Figure 1. Analysis of the species of gut microbiota and comparison of β-diversity index between the two groups of patients (AA1 and AA2). A. The PCoA diagrams of β-diversity at the family level for the two groups of patients. B. The results of the permutational multivariate analysis of variance (Adonis test) and analysis of similarities test. C. The heatmap of the species composition analysis for the two groups of patients. D. The bar plots of the species composition analysis for the two groups of patients. PCoA, principal coordinate analysis; AA1, Ann Arbor stage I-II; AA2, Ann Arbor stage III-IV.

that Akkermansia (P = 0.01) was more abundant in the HCDR group, while Parabacteroides distasonis (P = 0.03) was more abundant in the LCDR group (**Figure 4D-F**).

β2-microglobulin: Patients were categorized into the high β2-microglobulin group (≥ 2.7 μg/mL; n = 36) and low β2-microglobulin group (< 2.7 μg/mL; n = 33). There were no significant differences in α diversity between the two groups (P > 0.05) (Supplementary Figure 3). However, in the β diversity index, PCoA revealed distinct clustering patterns (**Figure 5A**), and the Adonis test confirmed significant differences (R^2 = 0.067, P = 0.041) (**Figure 5B**). Genus-level ROC curve analysis confirmed the discriminative power of key taxa, with AUC values exceeding 0.70 (**Figure 5C**). Comparison of species composition revealed that g_megamonas (P = 0.03) was more abundant in the high β2-microglobulin group, while g_roseburia (P = 0.04) and g_lachnospira (P = 0.02) were lower in this group compared to the low β2-microglobulin group (**Figure 5D-F**).

Extranodal organ involvement: Patients were divided into two groups: no extranodal involvement (OL1; n = 28) and extranodal involvement (OL2; n = 41). The Shannon index for α diversity was higher in the OL2 group compared to the OL1 group (**Figure 6A**). No significant differences were observed in Chao1 and Sob abundance curves between the groups. However, the Pielou index showed that the OL2 group was more homogeneous than the OL1 group. β diversity analysis revealed significant differences between the groups, with distinct clustering patterns observed in PCoA (**Figure 6B**). The Adonis test confirmed statistically significant differences (R^2 = 0.063, P = 0.032) (**Figure 6C**). Genus-level ROC curve analysis validated the discriminative power of key taxa, with AUC val-

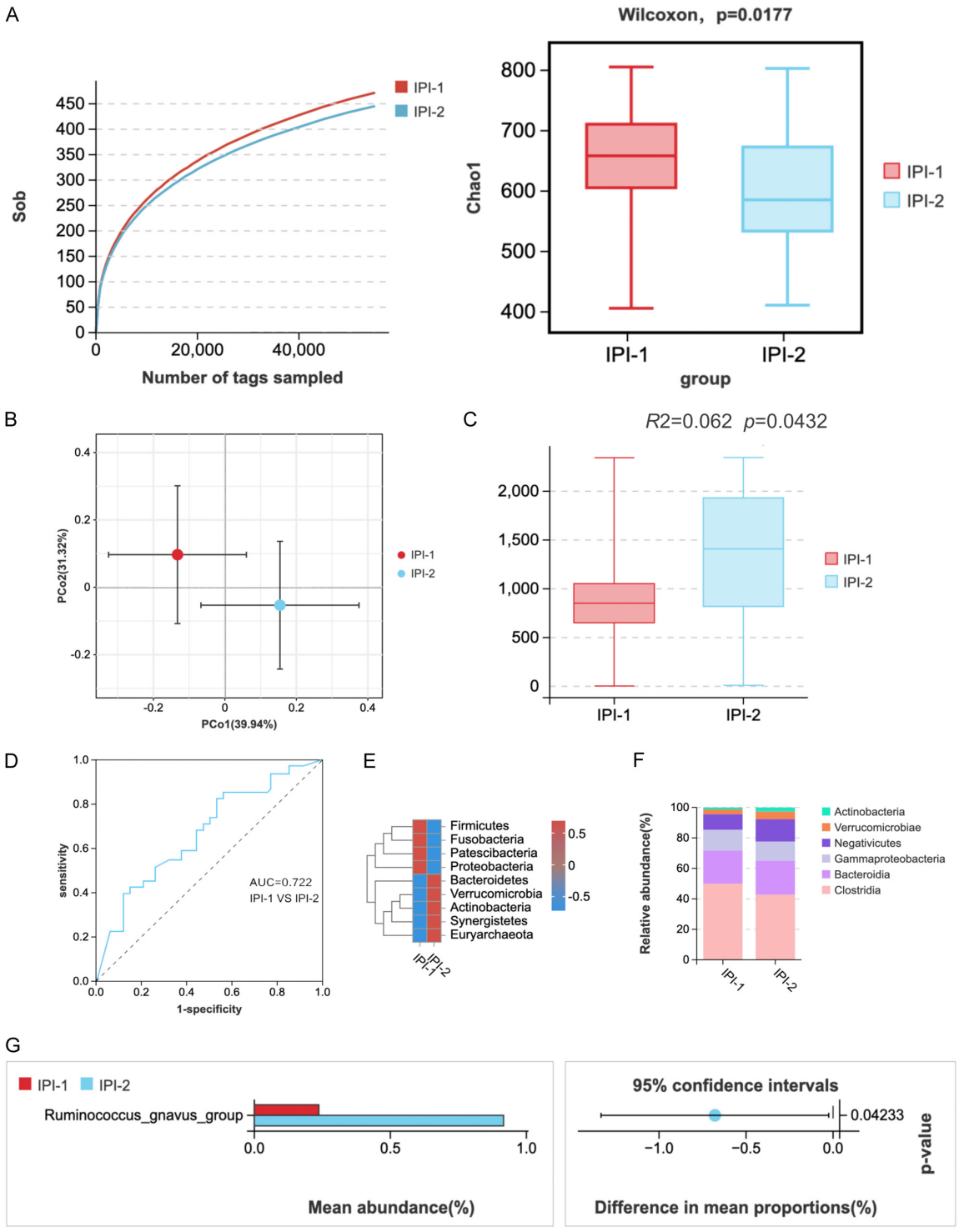

Figure 2. Analysis of the species of gut microbiota and comparison of α diversity index and β-diversity index between the two groups of patients (IPI-1 and IPI-2). A. α diversity index of species abundance in the IPI-1 and IPI-2 groups compared using the Wilcoxon test (P < 0.05). B. The PCoA diagram of β diversity in the IPI-1 and IPI-2 groups. C. The results of the Adonis test in the IPI-1 and IPI-2 groups. D. Genus-level ROC curve analysis. E. The heatmap of the species composition analysis for the two groups of patients. F. The bar plots of the species composition analysis for the two groups of patients. G. Differences at the genus level between the two groups of patients (IPI-1 & IPI-2). IPI, International Prognostic Index; PCoA, principal coordinate analysis; ROC, receiver operating characteristic.

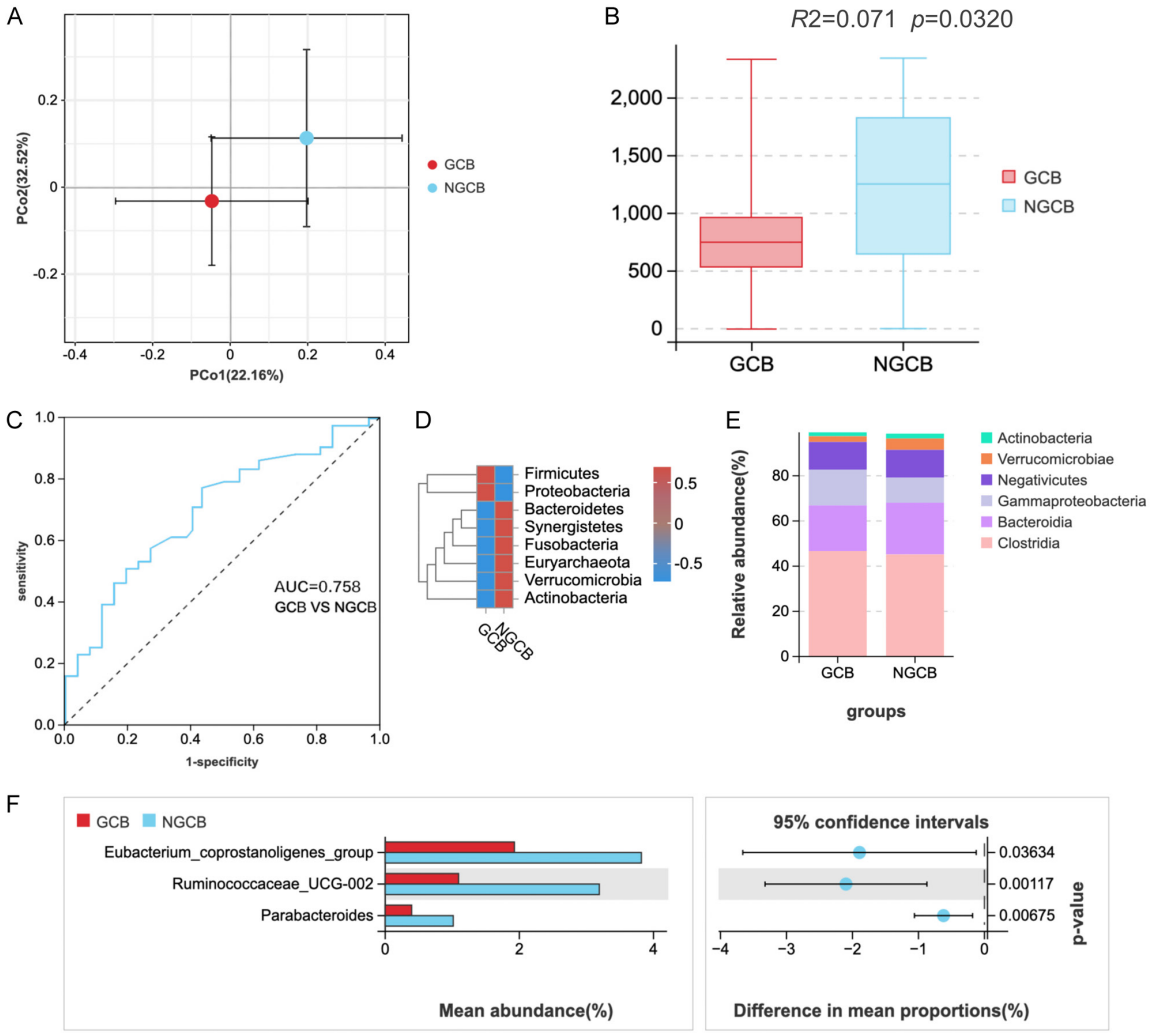

Figure 3. Analysis of the species of gut microbiota and comparison of β-diversity index between the two groups of patients (GCB and non-GCB). A. The PCoA diagrams of β diversity between the GCB and non-GCB groups. B. The results of the Adonis test and analysis of similarities test in β-diversity index. C. Genus-level ROC curve analysis. D. The heatmap of the species composition analysis for the two groups of patients. E. The bar plots of the species composition analysis for the two groups of patients. F. The differences at the genus level between the two groups of patients. GCB, germinal center B-cell-like; PCoA, principal coordinate analysis; ROC, receiver operating characteristic.

ues exceeding 0.70 (**Figure 6D**). Comparison of species composition revealed that Coprococcus (P = 0.04) and Alistipes indistinctus (P = 0.04) were more abundant in the OL2 group (**Figure 6E-G**). PD-1 levels were significantly lower in the OL2 group compared with the OL1 group (P < 0.05) (**Table 2**).

CR at the mid-term effectiveness evaluation: Patients were divided into two groups: S1 (patients with CR after four courses of RCHOP therapy, n = 38) and S2 (patients who failed to achieve CR after four courses, n = 31). No significant differences in α diversity were observed between the groups (P > 0.05) (Supplementary Figure 4). However, in the β diversity index, PCoA revealed distinct clustering patterns (**Figure 7A**), and the Adonis test confirmed significant differences (R^2 = 0.063, P = 0.032) (**Figure 7B**). Genus-level ROC curve analysis confirmed the discriminative power of key taxa, with AUC values exceeding 0.70 (**Figure 7C**). Comparison of species composition revealed that p_firmicutese (P < 0.01), g_ruminococcaceae_002 (P = 0.02), g_ruminococcaceae_005 (P = 0.03), and s_alistipes_indistinctus (P < 0.01) were more abundant in the S2 group (**Figure 7D-F**). Serum cytokine levels, including

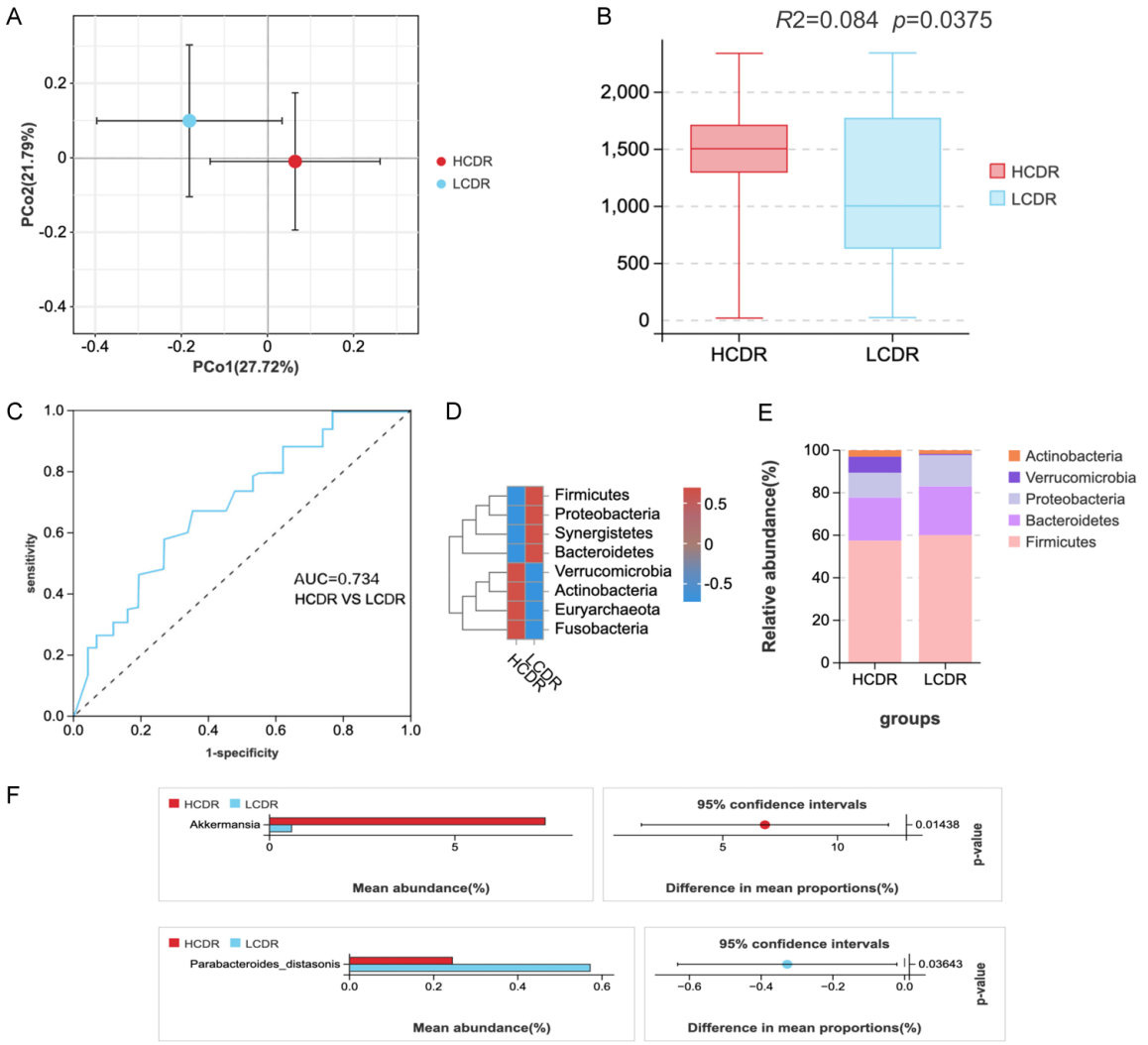

Figure 4. Analysis of the species of gut microbiota and comparison of β-diversity index between the two groups of patients (HCDR and LCDR). A. The PCoA diagrams of β diversity between the two groups. B. The results of the Adonis test and analysis of similarities test in β-diversity index. C. Genus-level ROC curve analysis. D. The heatmap of the species composition analysis for the two groups of patients. E. The bar plots of the species composition analysis for the two groups of patients. F. The differences at the genus level between the two groups of patients. HCDR, high CD4+/CD8+ ratio; LCDR, low CD4+/CD8+ ratio; PCoA, principal coordinate analysis; ROC, receiver operating characteristic.

interleukin-2 and interleukin-6, were significantly higher in the S1 group than in the S2 group (both $P < 0.05$) (**Table 3**).

Discussion

In recent years, research on the relationship between the gut microbiota and the development of lymphoma has attracted substantial attention. In this study, 16S rDNA gene sequencing of fecal samples was employed to investigate whether there are differences in the gut microbiota among DLBCL patients with diverse biological characteristics. The study found that differences in the gut microbiota exist among DLBCL patients with various biological features, which have been shown to be associated with prognosis. Therefore, alterations in the gut microbiota may be linked to the occurrence and progression of DLBCL.

To date, studies on intestinal dysbiosis in lymphoma patients have primarily focused on the diversity and structural changes in the gut microbiota in the context of autologous or allogeneic transplantation [16, 17]. However, there

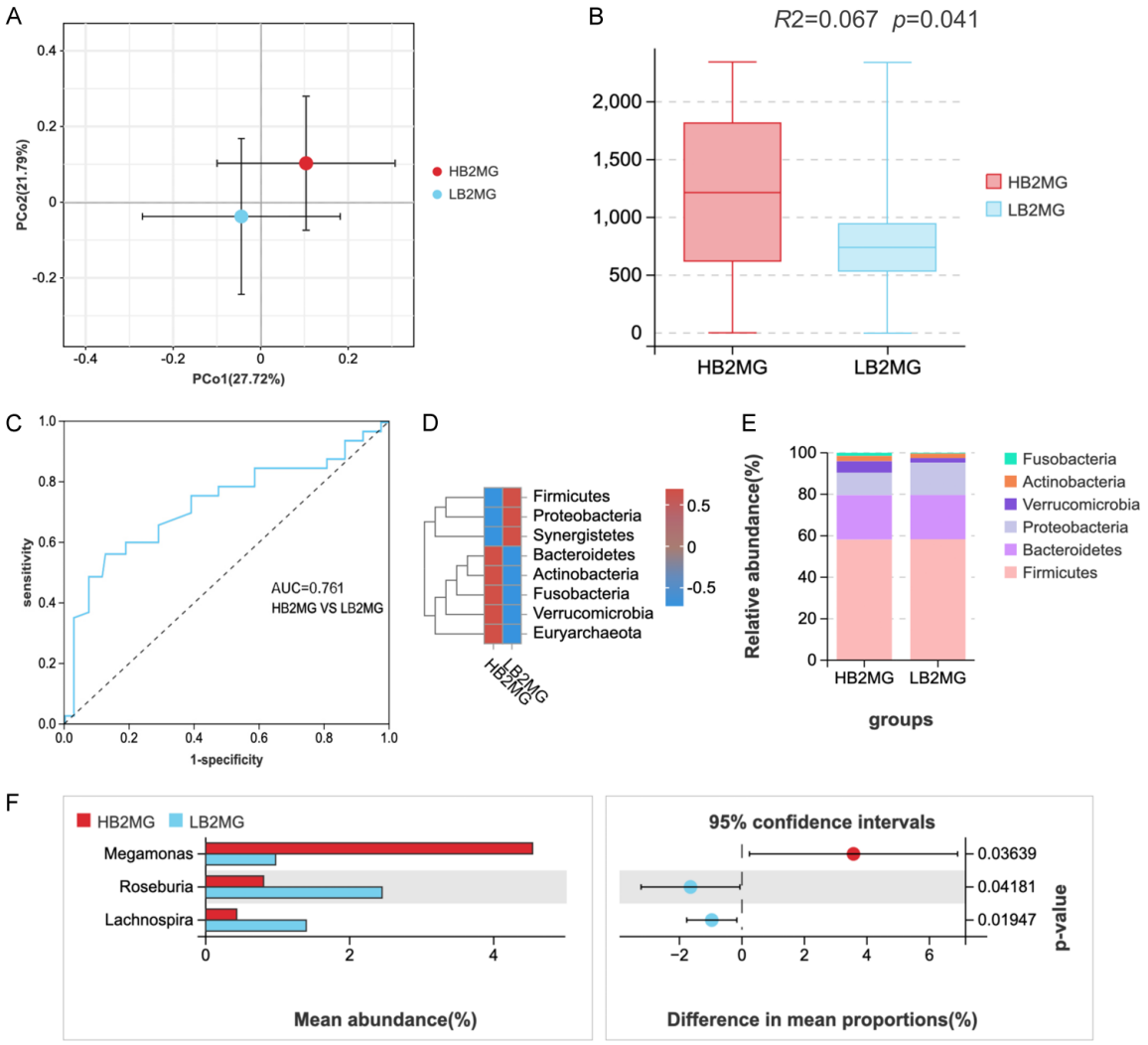

Figure 5. Analysis of the species of gut microbiota and comparison of β-diversity index between the two groups of patients (HB2MG and LB2MG). A. The PCoA diagrams of β diversity between the two groups. B. The results of the Adonis test and analysis of similarities test in β-diversity index. C. Genus-level ROC curve analysis. D. The heatmap of the species composition analysis for the two groups of patients. E. The bar plots of the species composition analysis for the two groups of patients. F. The differences at the genus level between the two groups of patients. HB2MG, high β2-microglobulin; LB2MG, low β2-microglobulin; PCoA, principal coordinate analysis; ROC, receiver operating characteristic.

are few studies directly examining lymphoma patients. For example, Diefenbach et al. [18] found no significant difference in the α-diversity index between lymphoma patients and healthy controls, but significant differences were observed in the β-diversity index. Similarly, Yuan et al. [19] reported no significant differences in α-diversity between DLBCL patients and healthy controls, while significant differences were noted in the β diversity index. In this study, there were no significant differences in α-diversity among most groups, with differences observed only in the International Prognostic Index (IPI) group and the group with extranodal involvement. In the IPI grouping, species abundance in the low IPI group was significantly higher than in the high IPI group, although there was no significant difference in species evenness between the two groups. This may be because different microbial communities can have similar functions. When the abundance of a microbial community with a specific function increases, other microbial communities with the same function remain unaffected, thus maintaining species evenness.

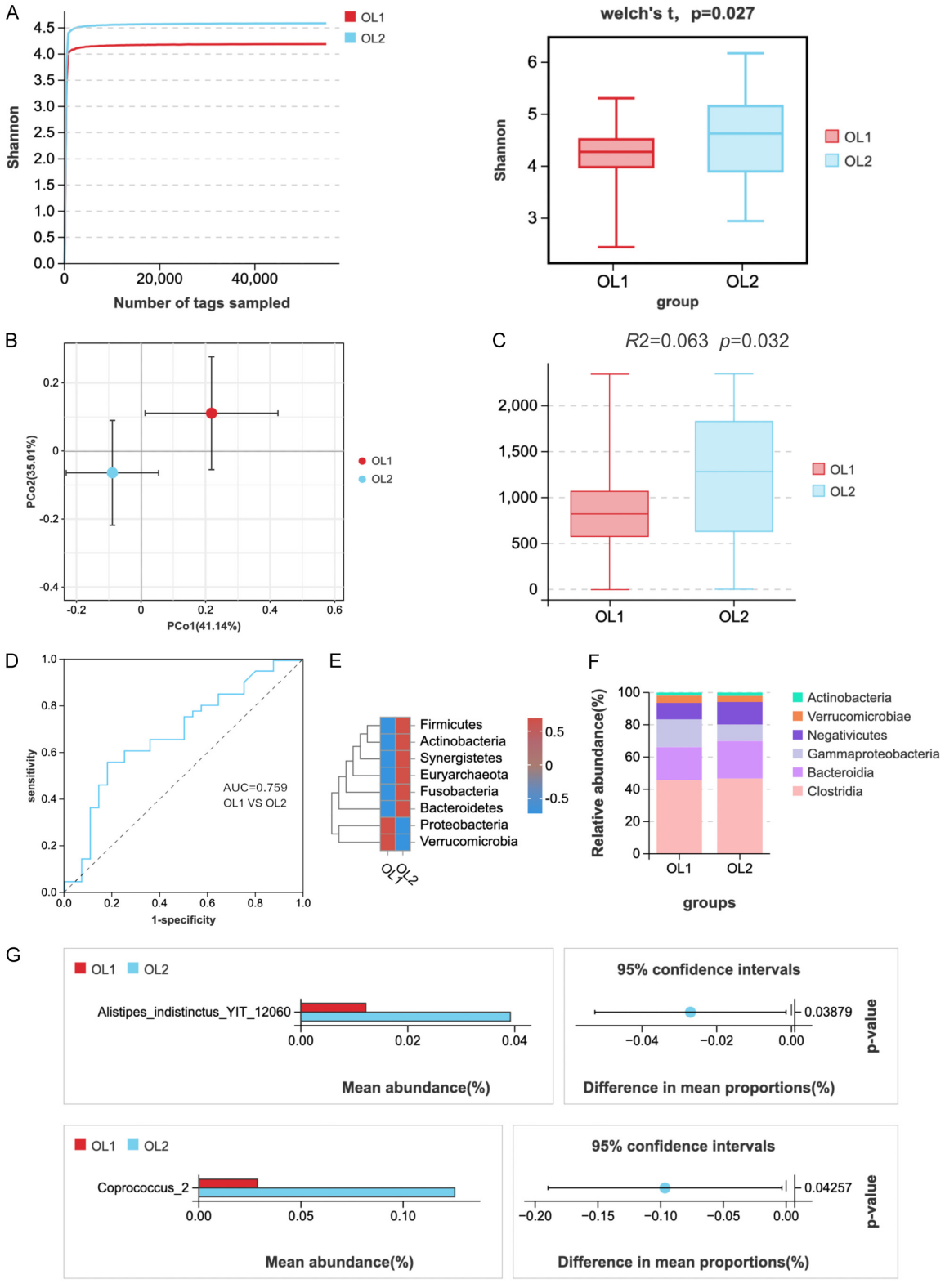

Figure 6. Analysis of the species of gut microbiota and comparison of α diversity index and β-diversity index between the two groups of patients (OL-1 and OL-2). A. In the α diversity index, the Shannon index of species between the two groups according to the Wilcoxon test ($P < 0.05$). B. The results of the Adonis test and analysis of similarities test in β-diversity index. C. The results of the Adonis test and analysis of similarities test in β-diversity index. D. Genus-level ROC curve analysis. E. The heatmap of the species composition analysis for the two groups of patients. F. The

bar plots of the species composition analysis for the two groups of patients. G. The differences at the genus level between the two groups of patients. OL-1, the no extranodal involvement group; OL-2, the extranodal involvement group; ROC, receiver operating characteristic.

Table 2. Comparison of serum cytokines, PD-1, and PD-L1 between the OL1 and OL2 groups

	OL1 (n = 28)	OL2 (n = 41)	Z	P
IL-2 (pg/mL)	0.770 (0.315, 2.205)	0.800 (0.345, 1.480)	-0.436	0.663
IL-6 (pg/mL)	24.130 (15.612, 36.885)	17.150 (7.190, 29.075)	-1.845	0.065
IL-10 (pg/mL)	5.980 (2.200, 35.357)	4.110 (2.415, 11.455)	-1.167	0.243
IFN-γ (pg/mL)	13.455 (6.815, 54.222)	8.950 (6.090, 33.635)	-0.642	0.521
TNF-α (pg/mL)	3.850 (2.120, 12.232)	3.950 (2.615, 9.250)	-0.049	0.961
PD-1 (pg/mL)	24.290 (8.492, 37.230)	6.810 (2.330, 17.130)	-3.01	0.003*
PD-L1 (pg/mL)	46.843 (27.930, 73.618)	55.711 (28.844, 79.290)	-0.379	0.705

IFN, interferon; IL, interleukin; OL1, no extranodal involvement; OL2, extranodal involvement; PD-1, programmed cell death protein 1; PD-L1, programmed death-ligand 1; TNF, tumor necrosis factor. *, $P < 0.05$.

Although this study did not directly compare the gut microbiota profiles of DLBCL patients to healthy controls, our findings align with previous observations of lymphoma-associated dysbiosis in comparable cohorts [18, 19]. To address this methodological gap and better delineate disease-specific microbial signatures, future studies should include age- and sex-matched healthy controls using standardized fecal collection protocols. This will enhance our ability to distinguish between DLBCL-specific alterations and confounding environmental or physiological variations.

An increasing body of evidence suggests that the gut microbiota plays a critical role in antitumor immunity and may contribute to the activation of immune checkpoint blockade therapies [20]. Targeting the biological characteristics of DLBCL patients through gut microbiota intervention, thereby mitigating the impact of gut microbiota imbalance on antitumor immunotherapy, may represent a promising approach to enhance immunotherapy efficacy. In this study, patients with DLBCL were grouped based on their clinical characteristics, and the microbiota composition of each group was analyzed. In the species analysis, the genus Megamonas was more abundant in patients with elevated β2-microglobulin levels compared to those with normal levels. One study revealed that Megamonas was significantly enriched in female patients with inactive systemic lupus erythematosus, with its abundance negatively correlating with C3 complement levels [21]. Another study showed that an increase in Megamonas in the gut was negatively correlated with the production of T-helper 17 cells, leading to a weakened immune response [22]. Previous studies have identified elevated β2-microglobulin as an independent prognostic factor associated with poor outcomes in DLBCL patients [23, 24].

It has also been shown that the abundance of Parabacteroides and Ruminococcus may be positively correlated with immune response [25]. In this study, these genera were significantly increased in patients with a poor prognosis, including those with a high-risk IPI score, non-GCB subtype, and non-CR status. These factors have been identified as independent predictors of poor prognosis. Therefore, whether patients with high abundance of these genera respond well to immunotherapy remains to be confirmed.

Eubacterium and Akkermansia have been shown to predict response to chimeric antigen receptor (CAR)-T cell therapy. The abundance of Akkermansia is associated with significantly elevated baseline peripheral T-cell levels, suggesting that gut microbiota intervention could potentially improve CAR-T cell therapy efficacy [25]. In this study, Akkermansia was found to be more abundant in the group with a high CD4+/CD8+ ratio compared to the low CD4+/CD8+ ratio group. Akkermansia can degrade mucins, releasing short-chain fatty acids (e.g., acetic acid and propionic acid), which in turn enhance cytokine release from effector T cells [26, 27]. In vitro experiments have shown that Akkermansia stimulates the release of the effector cytokine IFN-γ2 from CD4+ and CD8+

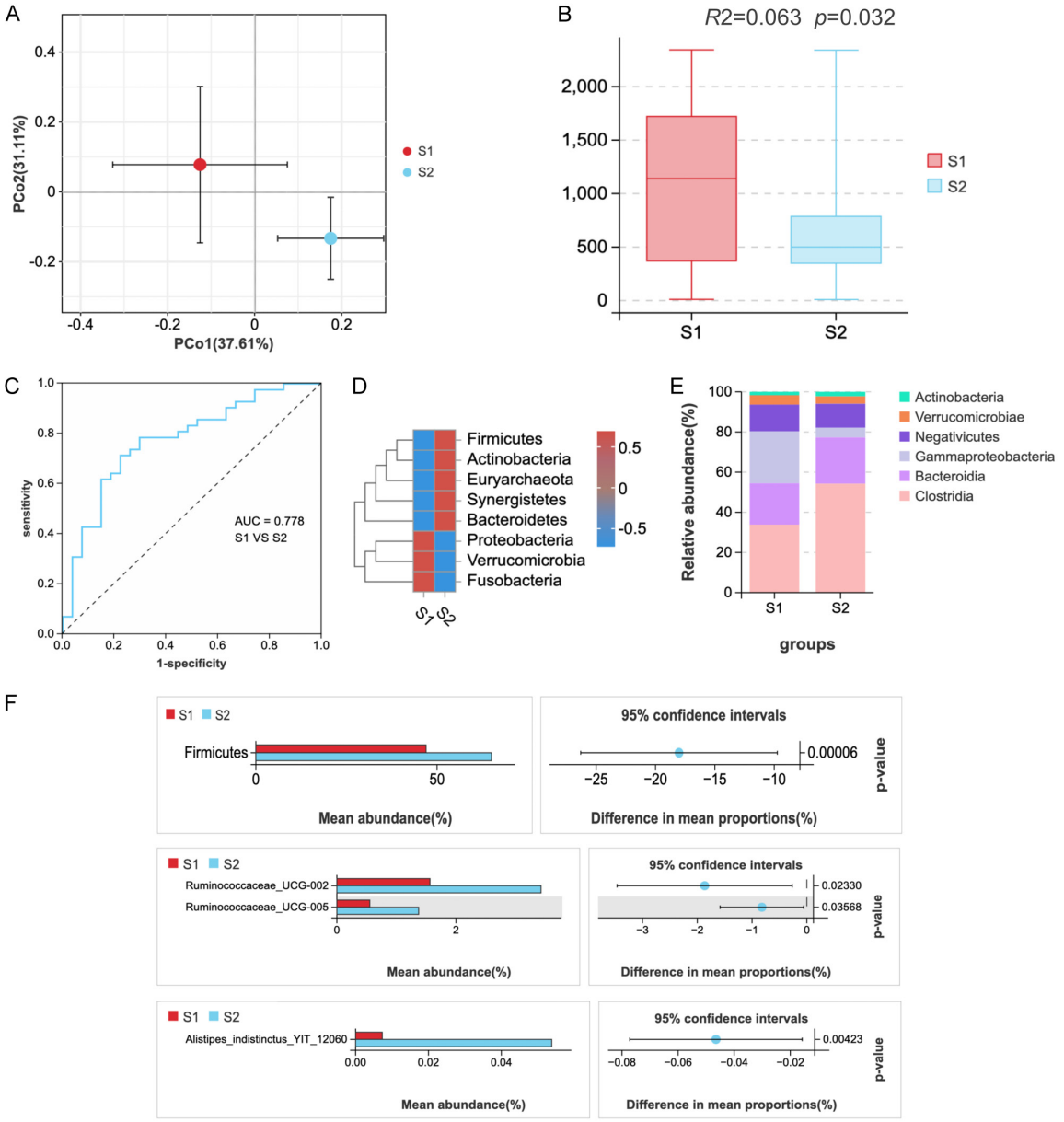

Figure 7. Analysis of the species of gut microbiota and comparison of β-diversity index between the two groups of patients (S1 and S2). A. The PCoA diagrams of β diversity between the two groups. B. The results of the Adonis test and analysis of similarities test in β-diversity index. C. Genus-level ROC curve analysis. D. The heatmap of the species composition analysis for the two groups of patients. E. The bar plots of the species composition analysis for the two groups of patients. F. The differences at the phylum, genus and species levels between the S1 and S2 groups. S1, CR after four courses of RCHOP therapy; S2, the failure to achieve a CR after four courses of RCHOP therapy; PCoA, principal coordinate analysis; ROC, receiver operating characteristic.

memory T cells, while lipids in the Akkermansia cell membrane activate the non-canonical TLR2-TLR1 pathway in immune cells [27]. Therefore, Akkermansia may increase the efficacy of CAR-T cell therapy, but further studies are needed to confirm this.

In a study evaluating the impact of antibiotic use on the gut microbiota in patients undergoing CAR-T cell therapy, it was hypothesized that high-risk patients requiring antibiotic treatment would exhibit certain characteristics, such as advanced disease stage and poor clinical status. These patients required antibiotic therapy to manage complications arising from infections [25]. However, some patients may not have clear evidence of infection, with increased antibiotic use due to disease confusion or mis-

Table 3. Comparison of serum cytokines, PD-1, and PD-L1 measurements between the CR and non-CR groups

	S1 group (n = 38)	S2 group (n = 31)	Z	P
IL-2 (pg/mL)	0.960 (0.442, 2.125)	0.480 (0.290, 1.120)	-2.437	0.015*
IL-6 (pg/mL)	24.350 (14.540, 38.625)	15.050 (7.190, 23.560)	-2.606	0.009*
IL-10 (pg/mL)	5.540 (2.475, 20.607)	4.690 (2.090, 11.290)	-0.850	0.395
IFN-γ (pg/mL)	13.455 (6.815, 54.222)	8.950 (6.090, 33.635)	-0.103	0.918
TNF-α (pg/mL)	4.490 (2.465, 11.212)	3.420 (2.520, 10.420)	-0.483	0.629
PD1 (pg/mL)	11.955 (2.345, 30.820)	13.320 (2.330, 21.420)	-0.611	0.541
PDL1 (pg/mL)	45.414 (27.539, 79.190)	57.921 (35.179, 73.726)	-0.778	0.436

The S1 group achieved CR after four courses of RCHOP therapy; the S2 group failed to achieve CR after four courses of RCHOP therapy. CR, complete remission; IFN, interferon; IL, interleukin; TNF, tumor necrosis factor; PD-1, programmed cell death protein-1; PD-L1, programmed death-ligand 1. *, $P < 0.05$.

diagnosis. It is critical to minimize such situations during clinical diagnosis and treatment.

Some studies showed that patients receiving antibiotics exhibited increased abundances of Enterococcus, Streptococcus, and Klebsiella, which led to microbial interference with peptidoglycan biosynthesis and the enrichment of antibiotic resistance-related genes [23, 25-28]. In this study, the abundance of Enterococcus was higher in the group with extranodal involvement (OL2) compared to the group without extranodal involvement (OL1). Previous research demonstrated that Enterococcus can translocate across the intestinal barrier into the mesenteric lymph nodes [29]. This bacterial genus has immune-stimulatory and proinflammatory effects, potentially causing significant inflammatory and immune-mediated damage to the intestine [29]. In our study, 26 out of 41 patients (63.4%) in the OL2 group with increased Enterococcus had lymphoma-associated intestinal injury. However, the relationship between Enterococcus abundance and intestinal injury requires further investigation.

Alteromonas, a relatively new genus within the phylum Bacteroidetes, is less commonly isolated compared to other bacteria in this phylum [30]. Studies have suggested that Alteromonas may play a role in colorectal cancer, exerting its effects through the interleukin-6/STAT3 pathway [31]. A recent study indicated that Alteromonas may positively influence tumor immunotherapy by altering the tumor microenvironment [32]. In another study, Alteromonas abundance increased in patients who responded well to nivolumab treatment for non-small cell lung cancer [30]. In the present study, Alteromonas abundance was higher in the group with extranodal involvement and the group that did not achieve CR after four courses of RCHOP therapy, compared to the no extranodal involvement group and the CR group. Additionally, these groups exhibited higher cytokine levels, including interleukin-2 and interleukin-6, as well as increased PD-1 and PD-L1 expression, compared with the no extranodal involvement and CR groups. We hypothesize that these patients may have a better response to immunotherapy. However, as there is currently no literature demonstrating the relationship between Alteromonas and lymphoma development or treatment, further studies are necessary to explore this association.

This study has several limitations. First, the study population was from North China, and their dietary habits may differ from those of individuals in other regions, potentially introducing bias in the gut microbiota composition. Therefore, caution should be exercised when generalizing the findings to other populations. Additionally, the influence of the gut microbiota may vary across different pathological subtypes of lymphoma. Further research is needed to explore the biological characteristics of the gut microbiota in relation to different lymphoma subtypes. Thirdly, this was a proof-of-concept study, and it remained unclear whether manipulating the gut microbiota can improve treatment responses or provide new strategies for potential lymphoma therapies. Therefore, future studies should aim to increase the sample size and expand the geographical scope to obtain a more precise understanding of the relationship between the gut microbiota and the development of lymphoma.

In conclusion, the composition and diversity of the gut microbiota in patients with DLBCL may be linked to the host's immune status, suggesting that the microbiota-immune axis may play a role in the occurrence and progression of lymphoma, thus affecting patient prognosis.

Acknowledgements

We would like to express our sincere gratitude to Kangsheng Zhu for their expert assistance in sample preparation. We are extremely thankful to our advisor, Yueping Liu, for her valuable insights, guidance, and continuous support throughout the research process. Her expertise and experience have been crucial in shaping this work. The present study was supported by the Medical Science Research Project of Hebei (grant no. 20221280).

Informed consent was obtained from all participants prior to their enrollment in the study.

Disclosure of conflict of interest

None.

Address correspondence to: Yueping Liu, Hebei Medical University Fourth Hospital, 12 Jiankang Road, Shijiazhuang 050000, Hebei, China. E-mail: liuyp@hebmu.edu.cn

References

[1] Ren C, Li Y, Li M and Wang Y. Unveiling vitamin C: a new hope in the treatment of diffuse large B-cell lymphoma (Review). Int J Oncol 2025; 66: 40.

[2] Shi Y, Han Y, Yang J, Liu P, He X, Zhang C, Zhou S, Zhou L, Qin Y, Song Y, Liu Y, Wang S, Jin J, Gui L and Sun Y. Clinical features and outcomes of diffuse large B-cell lymphoma based on nodal or extranodal primary sites of origin: analysis of 1,085 WHO classified cases in a single institution in China. Chin J Cancer Res 2019; 31: 152-161.

[3] Frontzek F and Lenz G. Novel insights into the pathogenesis of molecular subtypes of diffuse large B-cell lymphoma and their clinical implications. Expert Rev Clin Pharmacol 2019; 12: 1059-1067.

[4] Jelicic J, Juul-Jensen K, Bukumiric Z, Runason Simonsen M, Kragh Jørgensen RR, Roost Clausen M, Ludvigsen Al-Mashhadi A, Schou Pedersen R, Bjørn Poulsen C, Ortved Gang A, Brown P, El-Galaly TC and Stauffer Larsen T. Validation of prognostic models in elderly patients with diffuse large B-cell lymphoma in a real-world nationwide population-based study - development of a clinical nomogram. Ann Hematol 2025; 104: 433-444.

[5] Song JY, Perry AM, Herrera AF, Chen L, Skrabek P, Nasr MR, Ottesen RA, Nikowitz J, Bedell V, Murata-Collins J, Li Y, McCarthy C, Pillai R, Wang J, Wu X, Zain J, Popplewell L, Kwak LW, Nademanee AP, Niland JC, Scott DW, Gong Q, Chan WC and Weisenburger DD. Double-hit signature with TP53 abnormalities predicts poor survival in patients with germinal center type diffuse large B-cell lymphoma treated with R-CHOP. Clin Cancer Res 2021; 27: 1671-1680.

[6] Kamath HS, Shukla R, Shah U, Patel S, Das S, Chordia A, Satish P and Ghosh D. Role of gut microbiota in predisposition to colon cancer: a narrative review. Indian J Microbiol 2024; 64: 1-13.

[7] Moughnyeh MM, Brawner KM, Kennedy BA, Yeramilli VA, Udayakumar N, Graham JA and Martin CA. Stress and the gut-brain axis: implications for cancer, inflammation and sepsis. J Surg Res 2021; 266: 336-344.

[8] Chakrabarti A, Geurts L, Hoyles L, Iozzo P, Kraneveld AD, La Fata G, Miani M, Patterson E, Pot B, Shortt C and Vauzour D. The microbiota-gut-brain axis: pathways to better brain health. Perspectives on what we know, what we need to investigate and how to put knowledge into practice. Cell Mol Life Sci 2022; 79: 80.

[9] Clemente JC, Manasson J and Scher JU. The role of the gut microbiome in systemic inflammatory disease. BMJ 2018; 360: j5145.

[10] Khalil M, Di Ciaula A, Mahdi L, Jaber N, Di Palo DM, Graziani A, Baffy G and Portincasa P. Unraveling the role of the human gut microbiome in health and diseases. Microorganisms 2024; 12: 2333.

[11] Li S, Song J, Ke P, Kong L, Lei B, Zhou J, Huang Y, Li H, Li G, Chen J, Li X, Xiang Z, Ning Y, Wu F and Wu K. The gut microbiome is associated with brain structure and function in schizophrenia. Sci Rep 2021; 11: 9743.

[12] Lu H, Xu X, Fu D, Gu Y, Fan R, Yi H, He X, Wang C, Ouyang B, Zhao P, Wang L, Xu P, Cheng S, Wang Z, Zou D, Han L and Zhao W. Butyrate-producing Eubacterium rectale suppresses lymphomagenesis by alleviating the TNF-induced TLR4/MyD88/NF-κB axis. Cell Host Microbe 2022; 30: 1139-1150, e1137.

[13] Alaggio R, Amador C, Anagnostopoulos I, Attygalle AD, Araujo IBO, Berti E, Bhagat G, Borges AM, Boyer D, Calaminici M, Chadburn A, Chan JKC, Cheuk W, Chng WJ, Choi JK, Chuang SS, Coupland SE, Czader M, Dave SS, de Jong D, Du MQ, Elenitoba-Johnson KS, Ferry J, Geyer J, Gratzinger D, Guitart J, Gujral S, Harris M,

Harrison CJ, Hartmann S, Hochhaus A, Jansen PM, Karube K, Kempf W, Khoury J, Kimura H, Klapper W, Kovach AE, Kumar S, Lazar AJ, Lazzi S, Leoncini L, Leung N, Leventaki V, Li XQ, Lim MS, Liu WP, Louissaint A Jr, Marcogliese A, Medeiros LJ, Michal M, Miranda RN, Mitteldorf C, Montes-Moreno S, Morice W, Nardi V, Naresh KN, Natkunam Y, Ng SB, Oschlies I, Ott G, Parrens M, Pulitzer M, Rajkumar SV, Rawstron AC, Rech K, Rosenwald A, Said J, Sarkozy C, Sayed S, Saygin C, Schuh A, Sewell W, Siebert R, Sohani AR, Tooze R, Traverse-Glehen A, Vega F, Vergier B, Wechalekar AD, Wood B, Xerri L and Xiao W. The 5th edition of the World Health Organization classification of haematolymphoid tumours: lymphoid neoplasms. Leukemia 2022; 36: 1720-1748.

[14] Shi J, Geng C, Sang M, Gao W, Li S, Yang S and Li Z. Effect of gastrointestinal microbiome and its diversity on the expression of tumor-infiltrating lymphocytes in breast cancer. Oncol Lett 2019; 17: 5050-5056.

[15] Matzaras R, Nikopoulou A, Protonotariou E and Christaki E. Gut microbiota modulation and prevention of dysbiosis as an alternative approach to antimicrobial resistance: a narrative review. Yale J Biol Med 2022; 95: 479-494.

[16] Montassier E, Batard E, Massart S, Gastinne T, Carton T, Caillon J, Le Fresne S, Caroff N, Hardouin JB, Moreau P, Potel G, Le Vacon F and de La Cochetière MF. 16S rRNA gene pyrosequencing reveals shift in patient faecal microbiota during high-dose chemotherapy as conditioning regimen for bone marrow transplantation. Microb Ecol 2014; 67: 690-699.

[17] Montassier E, Gastinne T, Vangay P, Al-Ghalith GA, Bruley des Varannes S, Massart S, Moreau P, Potel G, de La Cochetière MF, Batard E and Knights D. Chemotherapy-driven dysbiosis in the intestinal microbiome. Aliment Pharmacol Ther 2015; 42: 515-528.

[18] Diefenbach CS, Peters BA, Li H, Raphael B, Moskovits T, Hymes K, Schluter J, Chen J, Bennani NN, Witzig TE and Ahn J. Microbial dysbiosis is associated with aggressive histology and adverse clinical outcome in B-cell non-Hodgkin lymphoma. Blood Adv 2021; 5: 1194-1198.

[19] Yuan L, Wang W, Zhang W, Zhang Y, Wei C, Li J and Zhou D. Gut microbiota in untreated diffuse large B cell lymphoma patients. Front Microbiol 2021; 12: 646361.

[20] Routy B, Gopalakrishnan V, Daillère R, Zitvogel L, Wargo JA and Kroemer G. The gut microbiota influences anticancer immunosurveillance and general health. Nat Rev Clin Oncol 2018; 15: 382-396.

[21] Balmant BD, Fonseca DC, Prudêncio APA, Rocha IM, Callado L, Alves JTM, Torrinhas RSMM, Borba EF and Waitzberg DL. Megamonas funiformis, plasma zonulin, and sodium intake affect C3 complement levels in inactive systemic lupus erythematosus. Nutrients 2023; 15: 1999.

[22] Li Y, Zhang SX, Yin XF, Zhang MX, Qiao J, Xin XH, Chang MJ, Gao C, Li YF and Li XF. The gut microbiota and its relevance to peripheral lymphocyte subpopulations and cytokines in patients with rheumatoid arthritis. J Immunol Res 2021; 2021: 6665563.

[23] Wu W, Miao L, Zhao L, Zhu Y, Mao J, Cai Z, Ji Y, Wang L, Wang Y and Jia T. Prognostic value of lactate dehydrogenase, serum albumin and the lactate dehydrogenase/albumin ratio in patients with diffuse large B-cell lymphoma. Hematology 2024; 29: 2293514.

[24] Zhao P, Zang L, Zhang X, Chen Y, Yue Z, Yang H, Zhao H, Yu Y, Wang Y, Zhao Z, Zhang Y and Wang X. Novel prognostic scoring system for diffuse large B-cell lymphoma. Oncol Lett 2018; 15: 5325-5332.

[25] Stein-Thoeringer CK, Saini NY, Zamir E, Blumenberg V, Schubert ML, Mor U, Fante MA, Schmidt S, Hayase E, Hayase T, Rohrbach R, Chang CC, McDaniel L, Flores I, Gaiser R, Edinger M, Wolff D, Heidenreich M, Strati P, Nair R, Chihara D, Fayad LE, Ahmed S, Iyer SP, Steiner RE, Jain P, Nastoupil LJ, Westin J, Arora R, Wang ML, Turner J, Menges M, Hidalgo-Vargas M, Reid K, Dreger P, Schmitt A, Müller-Tidow C, Locke FL, Davila ML, Champlin RE, Flowers CR, Shpall EJ, Poeck H, Neelapu SS, Schmitt M, Subklewe M, Jain MD, Jenq RR and Elinav E. A non-antibiotic-disrupted gut microbiome is associated with clinical responses to CD19-CAR-T cell cancer immunotherapy. Nat Med 2023; 29: 906-916.

[26] Dong C, Yu J, Yang Y, Zhang F, Su W, Fan Q, Wu C and Wu S. Berberine, a potential prebiotic to indirectly promote Akkermansia growth through stimulating gut mucin secretion. Biomed Pharmacother 2021; 139: 111595.

[27] Luu M, Riester Z, Baldrich A, Reichardt N, Yuille S, Busetti A, Klein M, Wempe A, Leister H, Raifer H, Picard F, Muhammad K, Ohl K, Romero R, Fischer F, Bauer CA, Huber M, Gress TM, Lauth M, Danhof S, Bopp T, Nerreter T, Mulder IE, Steinhoff U, Hudecek M and Visekruna A. Microbial short-chain fatty acids modulate CD8(+) T cell responses and improve adoptive immunotherapy for cancer. Nat Commun 2021; 12: 4077.

[28] Bae M, Cassilly CD, Liu X, Park SM, Tusi BK, Chen X, Kwon J, Filipčík P, Bolze AS, Liu Z, Vlamakis H, Graham DB, Buhrlage SJ, Xavier RJ and Clardy J. Akkermansia muciniphila phospholipid induces homeostatic immune responses. Nature 2022; 608: 168-173.

[29] Sardzikova S, Andrijkova K, Svec P, Beke G, Klucar L, Minarik G, Bielik V, Kolenova A and Soltys K. High diversity but monodominance of multidrug-resistant bacteria in immunocompromised pediatric patients with acute lymphoblastic leukemia developing GVHD are not associated with changes in gut mycobiome. Antibiotics (Basel) 2023; 12: 1667.
[30] Parker BJ, Wearsch PA, Veloo ACM and Rodriguez-Palacios A. The genus Alistipes: gut bacteria with emerging implications to inflammation, cancer, and mental health. Front Immunol 2020; 11: 906.
[31] Fu J, Li G, Li X, Song S, Cheng L, Rui B and Jiang L. Gut commensal Alistipes as a potential pathogenic factor in colorectal cancer. Discov Oncol 2024; 15: 473.
[32] Li B, Han Y, Fu Z, Chai Y, Guo X, Du S, Li C and Wang D. The causal relationship between gut microbiota and lymphoma: a two-sample Mendelian randomization study. Front Immunol 2024; 15: 1397485.

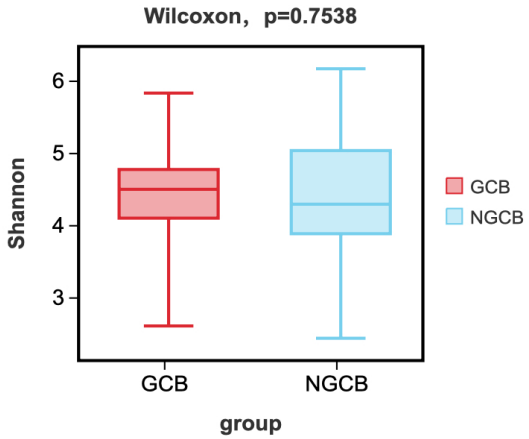

Supplementary Figure 1. Analysis of the species of gut microbiota and comparison of α-diversity index between the two groups of patients (GCB and non-GCB).GCB, germinal center B-cell-like.

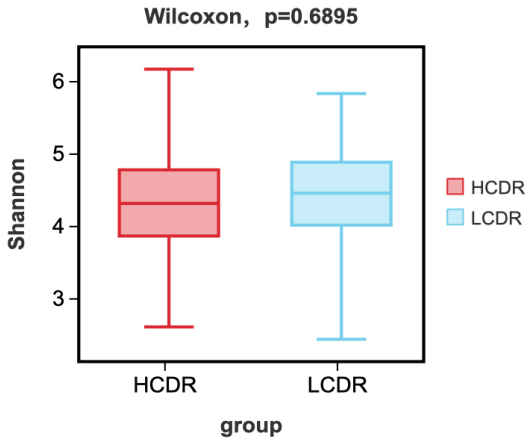

Supplementary Figure 2. Analysis of the species of gut microbiota and comparison of β-diversity index between the two groups of patients (HCDR and LCDR). HCDR, high CD4+/CD8+ ratio; LCDR, low CD4+/CD8+ ratio.

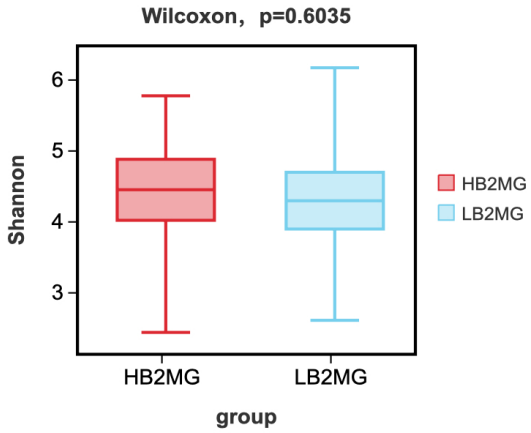

Supplementary Figure 3. Analysis of the species of gut microbiota and comparison of β-diversity index between the two groups of patients (HB2MG and LB2MG). HB2MG, high β2-microglobulin; LB2MG, low β2-microglobulin.

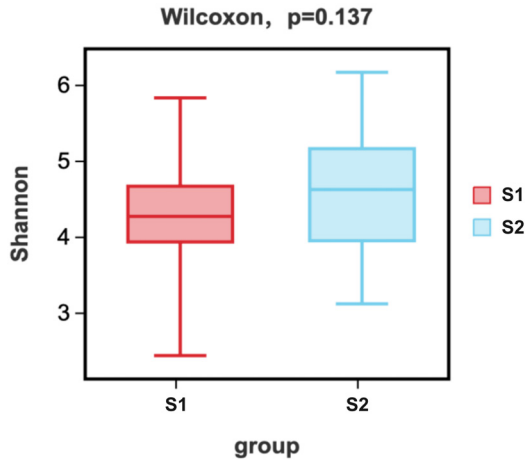

Supplementary Figure 4. Analysis of the species of gut microbiota and comparison of β-diversity index between the two groups of patients (S1 and S2). S1, CR after four courses of RCHOP therapy; S2, the failure to achieve a CR after four courses of RCHOP therapy.